Electron-phonon coupling in semiconductors by finite difference displacements

Pierre Lechifflart

February 2020

Contents

Chapter 1

Introduction

Thermal effects on the electronic band structure of solids due to electron-phonon interactions have been explored in the 1980's by Manuel Cardona *et al.* from both the experimental and theoretical sides using a perturbative approach in the electron-phonon interaction [1, 2].

This approach has been then extended to include dynamical effects [3, 4], more efficient sampling techniques [5, 6] and applied in the study of carrier lifetime, mobility, transport, kinks and satellites (for a review see Ref. [7]). Simultaneously with these perturbative approaches a new way to evaluate thermal effects emerged in the scientific literature : the use of finite difference displacements (FDD). Numerous efficient sampling techniques have been proposed in the literature [8, 9, 10] that allow a systematic study electronic properties at finite temperature.

These methods have two main advantages. First they are much more efficient than standard classical or path-integral molecular dynamics [11]. Second, finite difference displacements allow the calculation of thermal effects on observables that are difficult to treat within the perturbative approaches as for instance topological observables [12], nuclear magnetic response [13] or x-ray absorption near-edge structures [14].

The disadvantage of these approaches is that they require large supercells for the calculations to converge, and do not allow the inclusion of dynamical effects [4]. Thank to the FDD approach it was possible to investigate the correlations effects on electron-phonon coupling in bulk materials [15, 16] and finite systems [17]. In this work we apply the finite difference displacements proposed by some of the authors [10] to study thermal effects on the excitons in two systems: Silicon and two dimensional molybdenum disulfide. Thermal effects on the band gap have been studied since the 1950's, and recently it has also been shown that many-body correction to the band structure can strongly renormalize EPC, but little is known about the thermal effects on the exciton binding energy. For some systems, like hexagonal boron nitride, discordant results have been reported in the literature, some reporting blue shift and other red shift of excitons with temperature [18, 19]. In both these works electron-phonon coupling enters in

the Bethe-Salpeter equation as single-particle lifetimes, disregarding the fact that excitonic effects can strongly renormalize single-particle electron-phonon coupling matrix elements [20]. In other materials, as for example TiO2, some features in the absorption spectrum has been predicted to undergo a blueshift when increasing temperature while others shift to the red [21]. In monolayer black-phosphorus, experimental measurements show that excitons does not follow the usual Varshni's model [22], but blueshift with temperature [23]. Part of this behaviour may originate from the single-particle band structure due to the interplay between thermal expansion and electron-phonon coupling [24] or due to correlation effects [16]. But without a precise calculation it is very difficult to differentiate these effects from thermal behaviour of the excitonic binding energy. For this reason we decide to investigate it using finite difference displacement method that is easy to implement and to control. Finally it would be very useful to have a scheme for accounting coupling with phonons at the BSE level, in particular for polar semiconductors where an important renormalization of the binding energy was predicted and observed [25, 26]. Moreover, when only one excitonic peak is resolved in the experimental data, it is not easy to estimate the exciton binding energy, because the simple hydrogenic model is of no help [27].

Chapter 2

Theory

2.1 Density Functional Theory

In this work we make great use of the Density Functional Theory (DFT), developped at first by Hohenberg, Kohn and Sham in the 1960's. The first Hohenberg and Kohn theoren states that all the ground state properties of a many-electrons system are uniquely determined by its electronic density. So the Hamiltonian and the total ground state energy can be written as functionals of the ground state density : $\hat{H} = \hat{H}[n]$ and $E = E[n]$. Kohn and Sham [28] introduced a separation of the terms contributing to the total energy E, to map the study of the interacting system to the study of a simpler non interacting fictitious system. In the Kohn-Sham single particle scheme, the total energy of the interacting system is written as :

$$E[n] = T_{KS}[n] + E_H[n] + \int d\boldsymbol{r} n(\boldsymbol{r}) v_{ext}(\boldsymbol{r}) + E_{xc}[n] \tag{2.1}$$

where T_{KS} is the kinetic energy of a non interacting system with density n, E_H is the Hartree contribution to the total energy :

$$E_H[n] = \frac{1}{2} \int d^3r \int d^3r' \frac{n(r)n(r')}{|r - r'|}$$

and E_{xc} is the remaining part of the total energy which contains the exchange-correlation contributions and the difference in kinetic energy between the interacting system and the non-interacting system. Finally the Kohn-Sham equation write :

$$[-\frac{1}{2}\nabla^2 + v_{ext} + v_H + V_{xc}]\phi_i(\boldsymbol{r}) = \epsilon_i \phi_i(\boldsymbol{r}) \tag{2.2}$$

which is the equivalent of the Schrödinger equation for the non-interacting fictitious system. Its ground state density is by construction the same than the interacting system :

$$n(r) = \sum_i f_i |\phi_i(\vec{r})|^3 \tag{2.3}$$

with f_i being the occupation number of the state i. In Eq 2.2, $V_{xc} = \frac{\delta E_{xc}[n]}{\delta n}$ is the exchange and correlation potential of the interacting system, and v_{ext} is the same external potential than in Eq 2.1. It is now possible to solve the Kohn-Sham equations (Eq 2.2, Eq 2.3) self consistently and calculate the density of the interacting (real) system with Eq 2.1 if we approximate $E_{xc}[n]$. Once the density is known, it is possible to calculate the ground state energy of the interacting system and hence its ground state geometry.

There exists several methods to approximate the exchange-correlation energy functional. For example, the first one was proposed by Kohn and Sham in their original paper [28]. In principle, it is valid only for systems with slowly varying density. They called it the Local Density Approximation (LDA), and it is given by :

$$E_x^{LDA}c = \int d\boldsymbol{r} n(\boldsymbol{r}) \epsilon_{xc}^{heg}(n(r)) \tag{2.4}$$

where $\epsilon_{xc}^{heg}(n(r))$ is the exchange-correlation energy per electron of an homogeneous electron gas of density n. In this approximation, the exchange-correlation energy depends only on the local value of the density. This approximation is simple but has appeared to be very accurate to compute ground state properties of complex systems.

Another approximation is the Generalized Gradient Approximation (GGA), in which the energy functional depends also on the derivative of the density :

$$E_{xc}^{GGA} = \int dr f(n(r), \nabla_r n) \tag{2.5}$$

This generally yields more accurate results for heterogeneous electronic density. The approximation on the form of the energy functional is not the only one needed to compute quantities with DFT. The pseudopotentials are used to model the interaction between the positive ion and the electrons, in order to eliminate the singularity in the electrostatic potential of the nucleus, and the influence of core electrons. Indeed, core electrons are usually not involved in the chemical bonds and they act as a repulsive potential for the valence electrons. A pseudopotential replaces the nuclei and the core electrons and verifies several conditions : the effective and the original potential have the same value outside of a core region of radius r_c ; the effective valence wave functions are the same than the ones of a certain reference configuration of the original atom ; the energies of the valence states of the pseudoatom are the same than the ones of the original atom ; and in the core region, the pseudoatom wave functions do not have any nodes. The final requirement for a pseudopotential is to conserve the norm of the pseudo wave functions. In a periodic system, each electronic eigenfunction can be expressed as a sum of plane waves :

$$\psi_{n,k}(r) = \sum_G c_{n,k+G} e^{i(k+G)r} \tag{2.6}$$

where k is a vector in the reciprocal space that spans the first Brillouin zone, and G are the reciprocal lattice vectors. In practice, we need to cut this infinite

summation to be able to compute it. In fact, the Brillouin zone is sampled with a finite number of k points, and the summation over the G vectors is limited by a cutoff in the kinetic energy. It is assumed that the wave functions at the k points are representative of all the wave functions in the neighbourhood of the corresponding k point in the Brillouin zone. In practice we need to test for the convergence of the results depending on the number of k points.

To choose the cutoff in kinetic energy, the wave functions are approximated using only the coefficients below a threshold E_{cut} :

$$\frac{1}{2} \mid k+G \mid^2 \leq E_{cut} \tag{2.7}$$

Checking the convergence of results is needed to set this parameter as well.

2.1.1 Structure optimization

TODO:
1) Describe how forces are calculated in DFT
2) Describe the algoritm used to optimize the structure, the BFGS quasi-newton algorithm (see on WIKI)

2.2 Phonons

In this work we need to compute the normal modes of vibration of the crystals. Since each mode has its own wavelength and momentum, we call associate a quasi-particle that has the same wavelength and momentum to each mode, and these particles are called phonons. We study a chain of ions of mass M separated by a distance a, so that the Bravais lattice vectors are $\mathbf{R} = na$ with n an integer number. We note $u(na)$ the displacement of ion around it equilibrium position na. We assume the system to be under the harmonic approximation, with the potential energy arising only from first neighbors interaction, following Ashcroft-Mermin notations :

$$U^{harm} = \frac{1}{2} K \sum_n [u(na) - u([n+1]a)]^2$$

Where $K = \phi''(a)$, $\phi(x)$ being the interaction energy between two ions separated by a distance x. The equations of motion for the ions are given by Newton's second law :

$$M\ddot{u}(na) = \frac{\partial U^{harm}}{\partial u(na)} = -K\left[2u(na) - u([n-1]a) - u([n+1]a)\right], \tag{2.8}$$

These equations are the same than those of ions connected by massless springs with constant K. We assume Born-von Karman boundary conditions :

$$u([N+1]a) = u(a) \; ; \quad u(0) = u(Na)$$

It is as if the two ends of the chain of N ions were connected one to another with an extra spring. We are looking for solutions in the form :

$$u(na,t) \propto e^{i(kna-\omega t)} \tag{2.9}$$

They satisfy the boundary conditions :

$$e^{ikNa} = 1 \tag{2.10}$$

This implies that k has the form :

$$k = \frac{2\pi}{a}\frac{n}{N}, \quad \text{n an integer.}$$

We can see that the displacement $u(na)$ in 2.9 is unchanged by shifting k by $2\pi/a$. It means there are only N values of k that yield consistent solutions. We take them between $-\pi/a$ and π/a. This interval is called the First Brillouin Zone. One can show that the solutions are proportional to either the real or the imaginary part of the ansatz in 2.9 :

$$u(na,t) \propto \begin{Bmatrix} \cos(kna-\omega t) \\ \sin(kna-\omega t) \end{Bmatrix}$$

From these results we can derive a relation between ω and k which we call the dispersion relation :

$$\omega(k) = \sqrt{\frac{2K(1-coska)}{M}} = 2\sqrt{\frac{K}{M}}\left|\sin\frac{1}{2}ka\right|$$

The solutions in 2.2 describe waves propagating along the chain with phase velocity $c = \omega/k$, and group velocity $v = \partial\omega/\partial k$. We plot the dispersion curve in Figure 2.1. When k is small compared with π/a, ω is linear in k :

$$\omega = \left(a\sqrt{\frac{K}{M}}\right)|k| \tag{2.11}$$

Then the group velocity is the same as the phase velocity. However when the wavelength becomes short enough to be compared to the interparticle spacing, the dispersion relation is not linear anymore and it becomes flat when k reaches $\pm\pi/a$.

Now let us consider the same linear chain with two atoms per unit cell, with equilibrium positions na and $na+d$. We suppose $d \leq a/2$ so that the force between neighboring ions depends on whether they are separated by a distance d or $a-d$. We assume nearest neighbor interactions again, and that the force between two atoms in the same unit cell (separated by a distance d) is stronger. We write the harmonic potential energy like :

$$U^{harm} = \frac{K}{2}\sum_n [u_1(na) - u_2(na)]^2 + \frac{G}{2}\sum_n [u_2(na) - u_1([n+1]a)]^2, \tag{2.12}$$

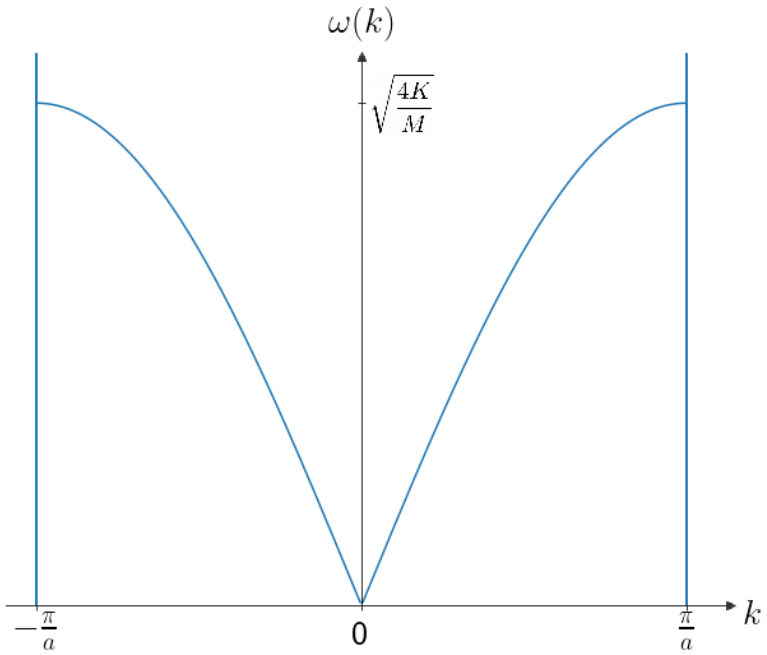

Figure 2.1: Dispersion curve for a mono-atomic linear chain with only nearest-neighbor interactions.

where u_1 and u_2 refer respectively to the first and the second ion in the unit cell, K and G are the spring constants with $K \leq G$. The equations of motion are :

$$\begin{aligned} M\ddot{u}_1(na) &= -\frac{\partial U^{harm}}{\partial u_1(na)} \\ &= -K[u_1(na) - u_2(na)] - G[u_1(na) - u_2([n+1]a)], \\ M\ddot{u}_2(na) &= -\frac{\partial U^{harm}}{\partial u_2(na)} \\ &= -K[u_2(na) - u_1(na)] - G[u_2(na) - u_1([n+1]a)] \end{aligned}$$

We seek solutions in the form of the following ansatz :

$$\begin{aligned} u_1(na) &= \epsilon_1 e^{i(kna-\omega t)}, \\ u_2(na) &= \epsilon_2 e^{i(kna-\omega t)}. \end{aligned}$$

They represent waves with angular frequency ω and wave vector k. ϵ_1 and ϵ_2 are unknown constants yet. Their ratio will determine the relative amplitude

and phase of the vibration of the ions within the unit cell. As in the mono-atomic case, the Born-von Karman boundary condition imply that the number of inequivalent value of k is N. The equations of motion transform to :

$$[M\omega^2 - (K+G)]\epsilon_1 + (K + Ge^{-ika})\epsilon_2 = 0,$$
$$(K + Ge^{ika})\epsilon_1 + [M\omega^2 - (K+G)]\epsilon_2 = 0.$$

This system of coupled equations have a solution if its determinant vanishes, *ie* :

$$[M\omega^2 - (K+G)]^2 = \left|K + Ge^{-ika}\right|^2 = K^2 + G^2 + 2KG\cos ka$$

The solutions of this equations are two positive values of ω that satisfy :

$$\omega^2 = \frac{K+G}{M} \pm \frac{1}{M}\sqrt{K^2 + G^2 + 2KG\cos ka} \tag{2.13}$$

And we obtain the amplitude ratio :

$$\frac{\epsilon_2}{\epsilon_1} = \mp \frac{K + Ge^{ika}}{|K + Ge^{ika}|}.$$

Then for each of the N values of k there are two solutions. The total of normal modes is $2N$, one per ion in the unit cell times the number of cells. We plot the dispersion curves for the two solutions of equation 2.13 in Figure 2.2. The lower branch is called the acoustic branch and has the same structure as the single branch in the mono-atomic case. The upper branch is called the optical branch.

We can characterize an acoustic mode as one in which all the atoms in a unit cell move in phase and the dynamics are dominated by the interaction between cells. An optical mode is one in which the ions within each unit cell are moving in a molecular vibratory mode, which is broadened by the intercellular interactions.

2.3 Density Functional Perturbation Theory

To compute the normal modes of vibration, we use Quantum ESPRESSO [29] which performs calculations in Density Functional Perturbation Theory (DFPT). TODO: Try to spend some more work on how it works DFTP

With this we can compute the second derivative of the ground-state energy E with respect to the displacements of the atoms $\mathbf{u}_s$:

$$\frac{\partial^2 E}{\partial \mathbf{u}_s \mathbf{u}_{s'}} = \int \frac{\partial^2 V(\mathbf{r})}{\partial \mathbf{u}_s \partial \mathbf{u}_{s'}} n(\mathbf{r}) d\mathbf{r} + \int \frac{\partial n(\mathbf{r})}{\partial \mathbf{u}_s} \frac{\partial V(\mathbf{r})}{\partial \mathbf{u}_{s'}} d\mathbf{r}.$$

In a generic three-dimensional crystal, it has the form of a matrix containing the interatomic force constants. From there we can solve the secular equation

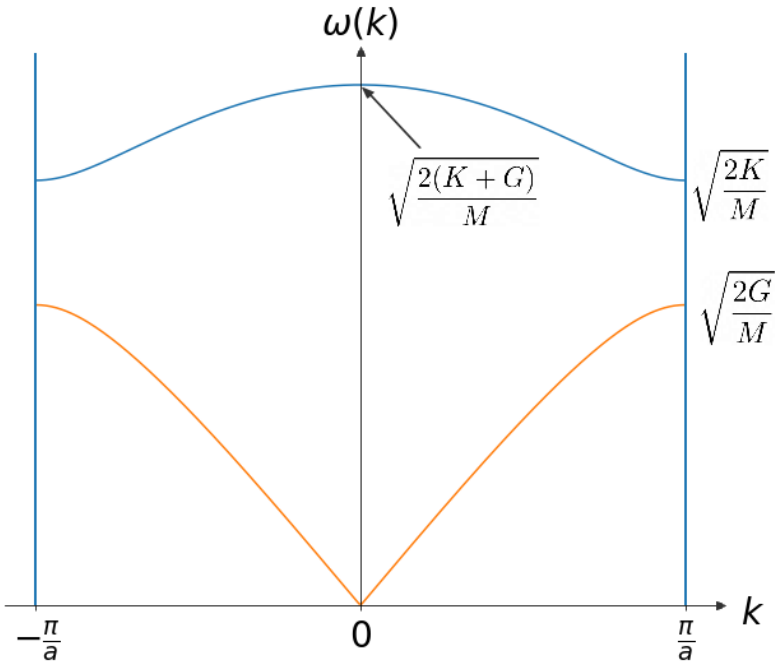

Figure 2.2: Dispersion curve for a diatomic linear chain. The orange curve is the acoustic branch and has the same structure as the single branch in the mono-atomic case. The blue curve is the optical branch.

which give us the normal mode frequencies ω and the eigenvectors $\mathbf{u}$:

$$\sum_{s'\beta} D_{s\alpha s'\beta}(\mathbf{q})\mathbf{u}_{s'\beta}(\mathbf{q}) = \omega_{\mathbf{q}}^2 \mathbf{u}_{s\alpha}(\mathbf{q})$$

Where

$$D_{s\alpha s'\beta}(\mathbf{q}) = \frac{1}{\sqrt{M_s M_{s'}}} \sum_{\nu} \frac{\partial^2 E_{tot}}{\partial \mathbf{u}_{\mu s\alpha} \partial \mathbf{u}_{\nu s'\beta}} e^{i\mathbf{q}(\mathbf{R}_\nu - \mathbf{R}_\mu)}$$

is the dynamical matrix of the crystal.$M_s, M_{s'}$ are the masses of atoms s and s'. μ and ν denote the number of the mode and α and β are two orthogonal directions. We can diagonalize this matrix to obtain the phonon modes at the point $\mathbf{q}$.

Chapter 3

Methods

TODO: write a small introduction on finite-difference methods for electron-phonon coupling and average of operator, have a look to: Bartomeu Monserrat 2018 J. Phys.: Condens. Matter30 083001

3.1 Average value of an operator at temperature T=0

Let $\hat{A}$ be an operator. Let $|\psi_0\rangle$ be the fundamental state of the harmonic oscillator. We want to compute the average of $\hat{A}$ ie $\langle\psi_0|\hat{A}|\psi_0\rangle$. In space representation the wave function of the fundamental state is

$$\psi_0(x) = \left(\frac{m\omega_0}{\pi\hbar}\right)^{1/4} \exp\left(-\frac{m\omega_0}{2\hbar}x^2\right).$$

Now we have :

$$\langle\psi_0|\hat{A}|\psi_0\rangle = \left(\frac{m\omega_0}{\pi\hbar}\right)^{1/2} \int_{-\infty}^{+\infty} dx \exp\left(-\frac{m\omega_0}{2\hbar}x^2\right) \hat{A}(x). \tag{3.1}$$

In order to compute this integral we expand $\hat{A}$ around $x = 0$:

$$\hat{A}(x) = \hat{A}(0) + x\frac{\partial\hat{A}}{\partial x}\Big|_{x=0} + \frac{1}{2}x^2\frac{\partial^2\hat{A}}{\partial x^2}\Big|_{x=0} + \mathcal{O}(x^3) \tag{3.2}$$

And we plug it in the integral (3.1). The term linear (as all the odd power terms) in x will vanish because it is multiplied by an even function in the integrand. We drop the term corresponding to the integration of $\hat{A}(0)$ because it is a constant, and we are left with :

$$\begin{aligned}\langle\psi_0|\hat{A}|\psi_0\rangle &= \left(\frac{m\omega_0}{\pi\hbar}\right)^{1/2} \frac{\partial^2\hat{A}}{\partial x^2}\Big|_{x=0} \int_{-\infty}^{+\infty} dx x^2 \exp\left(-\frac{m\omega_0}{2\hbar}x^2\right) + ... \\ &= \frac{1}{2}\frac{\hbar}{m\omega_0}\frac{\partial^2\hat{A}}{\partial x^2}\Big|_{x=0}\end{aligned}$$

Now if we assume the operator is purely quadratic *i.e* $\hat{A} = \frac{1}{2}x^2 \frac{\partial^2 \hat{A}}{\partial x^2}\Big|_{x=0}$, then there exists a value of x^* for which $\langle\psi_0|\hat{A}|\psi_0\rangle = \hat{A}(x^*)$, namely :

$$x^* = \pm\sqrt{\frac{\hbar}{m\omega_0}} \tag{3.3}$$

3.2 Average value of an operator at finite temperature T

In general at finite temperature T, the average of an operator writes :

$$\left\langle \hat{A}(T) \right\rangle = \frac{1}{\mathcal{Z}} \sum_n \langle E_n | \, \hat{A} \, | E_n \rangle \, e^{-\frac{E_n}{k_B T}}$$

where E_n is the energy associated with the eigenstate $|E_n\rangle$, $\mathcal{Z} = \sum_n e^{-\frac{E_n}{k_B T}}$ is the partition function and k_B is the Boltzmann constant. We will compute the average for the harmonic oscillator, whose eigenstates of the Hamiltonian are :

$$\psi_n(x) = \frac{1}{\sqrt{2^n n!}} \left(\frac{m\omega}{\pi\hbar}\right)^{1/4} e^{-\frac{m\omega}{2\hbar}x^2} H_n\left(\sqrt{\frac{m\omega}{\hbar}}x\right)$$

where H_n is the Hermite polynomial of order n. The energies associated with the eigenstates are :

$$E_n = \hbar\omega\left(n + \frac{1}{2}\right)$$

Using these, the average of operator $\hat{A}$ writes :

$$\left\langle \hat{A}(T) \right\rangle = \frac{1}{\mathcal{Z}} \sum_n e^{-\frac{\hbar\omega(n+1/2)}{k_B T}} \frac{1}{2^n n!} \int_{-\infty}^{+\infty} dx \sqrt{\frac{m\omega}{\pi\hbar}} \hat{A}(x) e^{-\frac{m\omega}{\hbar}x^2} H_n^2\left(\sqrt{\frac{m\omega}{\hbar}}x\right)$$

We do the change of variable $\sqrt{\frac{m\omega}{\hbar}}x = y$, so

$$\left\langle \hat{A}(T) \right\rangle = \frac{1}{\mathcal{Z}} \sum_n \frac{e^{-\frac{\hbar\omega(n+1/2)}{k_B T}}}{2^n n!\sqrt{\pi}} \int_{-\infty}^{+\infty} dy \hat{A}\left(\sqrt{\frac{\hbar}{m\omega}}y\right) e^{-y^2} H_n^2(y) \tag{3.4}$$

We compute it using the same kind of expansion than in (3.2). The operator assumes the same expansion both in x and y because the relation between the two variables is linear. Once again we will not keep the term in $\hat{A}(0)$ because it is just a constant. The term linear in y gives the following integral :

$$\frac{\partial \hat{A}}{\partial y}\Big|_{y=0} \int_{-\infty}^{+\infty} dy \; y H_n^2(y) e^{-y^2} \tag{3.5}$$

We use the following properties of the Hermite polynomials :

$$yH_n(y) = \frac{1}{2}H_{n+1}(y) + nH_{n-1}(y) \tag{3.6}$$

$$\implies yH_n^2(y) = \frac{1}{2}H_{n+1}(y)H_n(y) + nH_{n-1}(y)H_n(y) \tag{3.7}$$

and

$$\int_{-\infty}^{+\infty} dx H_n(x)H_m(x)e^{-x^2} = 2^n n!\sqrt{\pi}\delta_{n,m} \tag{3.8}$$

Finally the term linear in y of (3.5) vanishes using (3.7) and (3.8). To compute the term in y^2, we use the same property than in (3.7) :

$$y^2H_n^2(y) = \frac{1}{4}H_{n+1}^2(y) + n^2H_{n-1}^2(y) + nH_{n+1}(y)H_{n-1}(y) \tag{3.9}$$

The term in y^2 in (3.4) becomes, making use of (3.8) and (3.9) :

$$\frac{1}{2}\frac{\partial^2\hat{A}}{\partial y^2}\Big|_{y=0}\int_{-\infty}^{+\infty} dy\ y^2H_n^2(y)e^{-y^2} = \frac{1}{2}\frac{\partial^2\hat{A}}{\partial y^2}\Big|_{y=0}\sqrt{\pi}2^n n!\left(n+\frac{1}{2}\right)$$

Equation (3.4) becomes :

$$\left\langle \hat{A}(T)\right\rangle = \frac{1}{2}\frac{\partial^2\hat{A}}{\partial y^2}\Big|_{y=0}\frac{1}{\mathcal{Z}}\sum_n e^{-\frac{\hbar\omega(n+1/2)}{k_BT}}\left(n+\frac{1}{2}\right) \tag{3.10}$$

Now we take a look at the partition function $\mathcal{Z}$ in the case of the harmonic oscillator :

$$\frac{1}{\mathcal{Z}} = \frac{1}{\sum_n e^{-\frac{\hbar\omega\left(n+\frac{1}{2}\right)}{k_BT}}} = e^{\frac{\hbar\omega}{2k_BT}}\left(1-e^{-\frac{\hbar\omega}{k_BT}}\right),$$

by properties of the geometric series. The latter also give the result :

$$\sum_n e^{-\frac{\hbar\omega(n+1/2)}{k_BT}}\left(n+\frac{1}{2}\right) = e^{-\frac{\hbar\omega}{2k_BT}}\left[\frac{1}{2\left(1-e^{-\frac{\hbar\omega}{k_BT}}\right)} + \frac{e^{-\frac{\hbar\omega}{k_BT}}}{\left(1-e^{-\frac{\hbar\omega}{k_BT}}\right)^2}\right]$$

If we come back to the original variable x with $\frac{\partial^2\hat{A}}{\partial y^2} = \frac{\hbar}{m\omega}\frac{\partial^2\hat{A}}{\partial x^2}$, the average of operator $\hat{A}$ is given by :

$$\left\langle \hat{A}(T)\right\rangle = \frac{\hbar}{2m\omega}\frac{\partial^2\hat{A}}{\partial y^2}\Big|_{y=0}\left(\frac{1}{2}+n_B(\omega,T)\right),$$

where $n_B(\omega,T) = (e^{\hbar\omega/k_BT}-1)^{-1}$ is the Bose-Einstein function. Similarly than in the previous section, we would like to find a value x^* for which $\left\langle \hat{A}(T)\right\rangle = \hat{A}(x^*)$. If we assume $\hat{A}$ to be purely quadratic, *i.e* $\hat{A}(x) = \frac{1}{2}\frac{\partial^2\hat{A}}{\partial x^2}\Big|_{x=0}$, then

$$x^*(T) = \pm\sqrt{\frac{\hbar}{m\omega}\left(\frac{1}{2}+n_B(\omega,T)\right)}$$

These are two displacements induced by one mode of vibration at a given temperature. Now to compute the average of the operator, we need to displace all atoms along each vibration mode according to those displacements. Here is the formula from Zacharias and Giustino [9] that gives the displacement Δr_{sa} (s and a indicate the atom and the Cartesian direction, respectively):

$$\Delta r_{sa} = \sqrt{\frac{\hbar}{M_s \omega_\nu}} \sum_\nu (-1)^{\nu-1} \sqrt{1 + 2n_B(\omega_\nu, T)}\, \epsilon_{sa,\nu}, \tag{3.11}$$

where M_s is the mass of the s-th atom, ω_ν is the pulsation of the ν-th mode and $\epsilon_{sa,\nu}$ is the eigenvector associated to this vibration mode. Note the sign alternates between plus and minus in the sum. This is one possibility chosen by Zacharias and Giustino. Another choice was made by Monserrat in [8]. His approach is to average over all the possible sign combinations, which he calls thermal lines. This is supposed to yield more precise results but is slower to converge.

3.3 Mapping phonons in a supercell

As seen before, we need to compute the electronic properties by finite displacements in supercells to have more accurate results. However the computation of phonons in supercell is highly time consuming. Hence we use the following method to map phonons computed in a unit cell to supercells. We follow the notation of Ashcroft-Mermin Chapt. 22 [30] and write the solutions of the harmonic problem in periodic systems within the Born-von Karman boundary conditions as:

$$u_\mu(\mathbf{q}, t) = \epsilon_\mu e^{i(\mathbf{qR} - \omega t)} \tag{3.12}$$

where the complex eigenvectors of the dynamical matrix are calculated by means of DFTP and $\mathbf{q}$ is a regular point grid in the first Brillouin zone, and $\omega^\nu_{\mathbf{q}}$ are the eigenvalues. The number and the length of the ϵ_μ vectors is equal to $3 \cdot N$, where N is the number of atoms in the unit cell. Suppose we have a regular grid of q-points (n_{qx}, n_{qy}, n_{qz}) for a total of $n_{\mathbf{q}} = n_{qx} \cdot n_{qy} \cdot n_{qz}$. This mode can be mapped in real-space in a supercell of size (n_{qx}, n_{qy}, n_{qz}). In order to map the phonons first of all we contruct the new eigenvalues and eigenvectors $\tilde{\omega}, \tilde{\epsilon}$. The eigenvalues can be easily constructed as:

$$\tilde{\omega} = \begin{pmatrix} \omega_{q_1} \\ \omega_{q_2} \\ \vdots \\ \omega_{q_{n\mathbf{q}}} \end{pmatrix}$$

For the eigenvectors we divide the procedure in two steps. First we construct

eigenvectors without phase correction as:

$$\tilde{\epsilon}_{\mu+\mathbf{q}_1} = \begin{pmatrix} \epsilon^{\mu}_{\mathbf{q}_1} \\ \epsilon^{\mu}_{\mathbf{q}_1} \\ \vdots \\ \epsilon^{\mu}_{\mathbf{q}_1} \end{pmatrix}, ..., \tilde{\epsilon}_{\nu+\mathbf{q}_2} = \begin{pmatrix} \epsilon^{\nu}_{\mathbf{q}_2} \\ \epsilon^{\nu}_{\mathbf{q}_2} \\ \vdots \\ \epsilon^{\nu}_{\mathbf{q}_2} \end{pmatrix}$$

where the vectors $\epsilon^{\mu}_{\mathbf{q}}$ are defined in the unit cell and they have the dimension of $3 \cdot N$ while the vectors $\tilde{\epsilon}_{\mu}$ are in the supercell and they have dimension $(3 \cdot N \cdot n_{\mathbf{q}})$. In the unit cell there are $3N$ eigenvectors for each q-point, while in the supercell there are $3N \cdot n_{\mathbf{q}}$ for a single q-point, the same number in both cases. Notice that we have copied the same eigenvector for each of the cell that compose the supercell. Now we have have to apply the phase factor of Eq. 3.12 as:

$$\tilde{\epsilon}_{\mu+\mathbf{q}_1} = \begin{pmatrix} \epsilon^{\mu}_{\mathbf{q}_1} \cdot e^{i\mathbf{q}_1 R_1} \\ \epsilon^{\mu}_{\mathbf{q}_1} \cdot e^{i\mathbf{q}_1 R_2} \\ \vdots \\ \epsilon^{\mu}_{\mathbf{q}_1} \cdot e^{i\mathbf{q}_1 R_N} \end{pmatrix}$$

where the R_N are the translation vectors that generate the different cells that form the supercell, starting from the unit cell. In the part care should be taken because the order of the cells must be the same for the atomic structure and polarization vectors. Finally, since there is an arbitrarity in the choice of the eigenvector phase, we can consider only the real-part of these vectors.

$$\tilde{\epsilon}_{\mu+\mathbf{q}_1} = \begin{pmatrix} Re\left[\epsilon^{\mu}_{\mathbf{q}_1} \cdot e^{i\mathbf{q}_1 R_1}\right] \\ Re\left[\epsilon^{\mu}_{\mathbf{q}_1} \cdot e^{i\mathbf{q}_1 R_2}\right] \\ \vdots \\ Re\left[\epsilon^{\mu}_{\mathbf{q}_1} \cdot e^{i\mathbf{q}_1 R_N}\right] \end{pmatrix}$$

Chapter 4

Results

4.1 Materials

TODO:
1) describe each material BN, phosphorene, Polyacetilene 2) Put band strcture of the materials, say how much is the gap if it is polar or not etc.. put a figure for each material 3) describe the optimization of the structure, put the cell you used to simulate each systems and the optimized atomic positions put the table with all your results and the different methods

4.2 Gap renormalization

TODO: Put the table you have done with all results and the different methods you used, then comment the different table and results
We applied these methods to several materials, including polyethylene, hexagonal Boron Nitride and a single layer of Phosphorene in α phase, also known as Black Phosphorus. We performed the phonon calculations in Quantum ESPRESSO [29] to obtain the eigenmodes of the monolayer with a single unit cell. After performing a mapping of phonons as described in the previous section, we computed the correction of the direct gap due to thermal effects. We increased the size of the supercells we used and checked for the convergence of the electronic gap correction.

For materials containing different types of atoms such as polyethylene or hexagonal Boron Nitride, our method did not converge because of the atoms having different charges and therefore the optical phonon modes induce long-range dipole forces that require very large supercells to converge [31]. Moreover for the particular case of hBN, Monserrat *et al.* stated that we would need a 32x32x32 supercell to reach convergence, which is virtually impossible for us [32]. Fig. 4.1 is the example of polyethylene, where we see that there is no convergence within the range of supercell sizes we use.

The example of black phosphorus is displayed in Fig. 4.2. We can see that

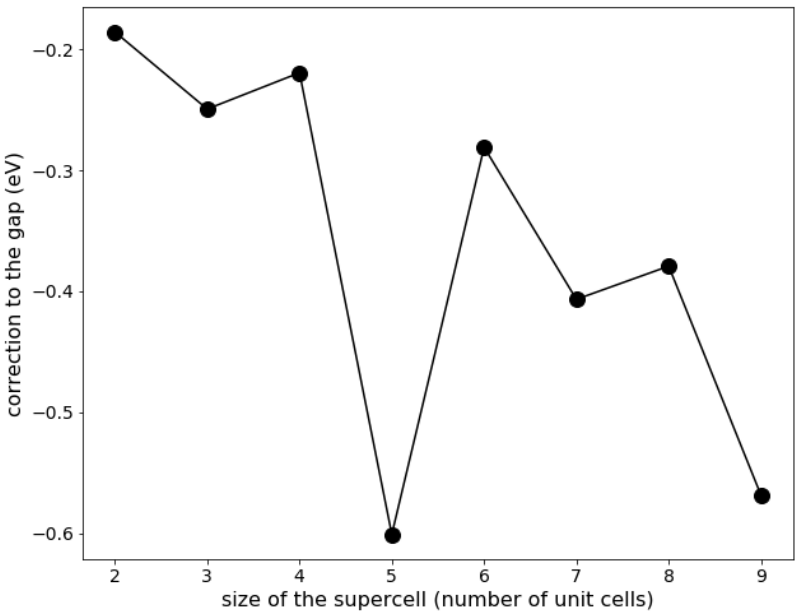

Figure 4.1: Example of polyethylene. Correction to the gap with respect to the size of the supercell. Since polyethylene is a linear chain, the supercells are just a given number of juxtaposed unit cells.

unlike the previous example convergence can be reached for Black-Phososhorous. This is due to the fact that BP is not a polar material and there are no long-range forces.Unfortunately, we found that the correction to the gap in the two-dimensional BP, that is already small in the bulk [24], goes to zero for large supercells.

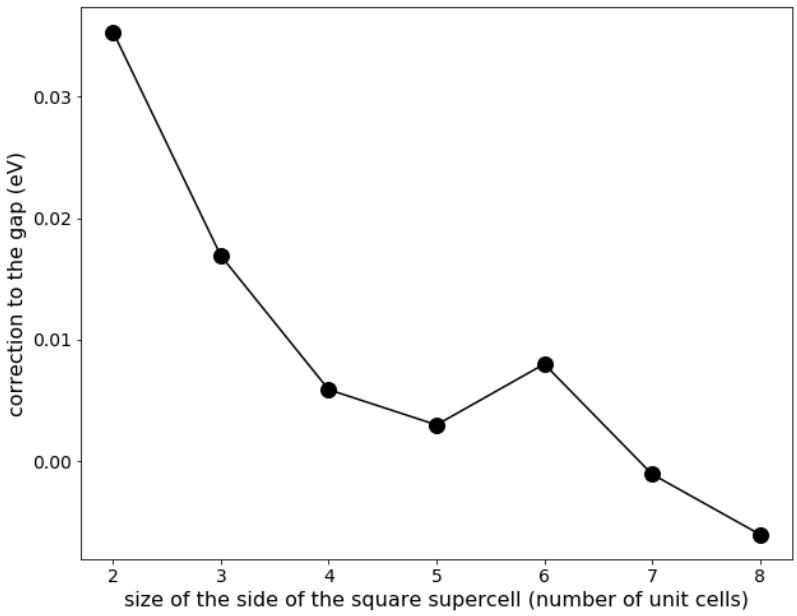

Figure 4.2: Example of black phosphorus. Correction to the gap with respect to the size of the supercell. The supercells are squares of a given number of unit cells.

Chapter 5

Conclusion

In this work I presented the derivation of the method used in our calculations : the fact that a physical quantity at temperature T can be obtained by the thermal average of the corresponding operator on particular atomic configurations at that temperature. We computed the thermal averages by finite displacement differences. We used different supercell sizes to check for convergence of the results, and we developped a method to map phonons computed in a unit cell to any supercell, reducing the time cost of the calculations.

We applied the method to several materials and we saw a convergence of the correction to electronic gap in the case of black phosphorus.

Future work would be to tune the method to obtain significant results for polar materials, as well as accounting for excitonic effects alongside thermal effects in the correction of physical quantities.

Due to the COVID-19 crisis and the quarantine in France, the internship I made to work on this project was only six weeks long and I had to work from home which made progress more difficult.

Chapter 6

Acknowledgments

I thank Claudio Attaccalite for his supervision of this internship and Alexandre Zappelli for the management of the computer cluster Rosa on which I performed most of the calculations. I thank the TSN team at CINaM for their warm welcome.

Bibliography

[1] PB Allen and M Cardona. Temperature dependence of the direct gap of si and ge. *Physical review B*, 27(8):4760, 1983.

[2] Philip B Allen and Volker Heine. Theory of the temperature dependence of electronic band structures. *Journal of Physics C: Solid State Physics*, 9(12):2305, 1976.

[3] Elena Cannuccia and Andrea Marini. Effect of the quantum zero-point atomic motion on the optical and electronic properties of diamond and trans-polyacetylene. *Physical review letters*, 107(25):255501, 2011.

[4] Gabriel Antonius, Samuel Poncé, E Lantagne-Hurtubise, Gabriel Auclair, Xavier Gonze, and Michel Côté. Dynamical and anharmonic effects on the electron-phonon coupling and the zero-point renormalization of the electronic structure. *Physical Review B*, 92(8):085137, 2015.

[5] Kristen Kaasbjerg, Kristian S Thygesen, and Karsten W Jacobsen. Phonon-limited mobility in n-type single-layer mos 2 from first principles. *Physical Review B*, 85(11):115317, 2012.

[6] Samuel Poncé, Elena R Margine, Carla Verdi, and Feliciano Giustino. Epw: Electron–phonon coupling, transport and superconducting properties using maximally localized wannier functions. *Computer Physics Communications*, 209:116–133, 2016.

[7] Feliciano Giustino. Electron-phonon interactions from first principles. *Reviews of Modern Physics*, 89(1):015003, 2017.

[8] Bartomeu Monserrat. Vibrational averages along thermal lines. *Phys. Rev. B*, 93:014302, Jan 2016.

[9] Marios Zacharias and Feliciano Giustino. One-shot calculation of temperature-dependent optical spectra and phonon-induced band-gap renormalization. *Phys. Rev. B*, 94:075125, Aug 2016.

[10] Marios Zacharias and Feliciano Giustino. Theory of the special displacement method for electronic structure calculations at finite temperature. *Physical Review Research*, 2(1):013357, 2020.

[11] Rafael Ramírez, Carlos P Herrero, Eduardo R Hernández, and Manuel Cardona. Path-integral molecular dynamics simulation of 3 c- si c. *Physical Review B*, 77(4):045210, 2008.

[12] Bartomeu Monserrat and David Vanderbilt. Temperature effects in the band structure of topological insulators. *Physical Review Letters*, 117(22):226801, 2016.

[13] Jean-Nicolas Dumez and Chris J Pickard. Calculation of nmr chemical shifts in organic solids: Accounting for motional effects. *The Journal of chemical physics*, 130(10):104701, 2009.

[14] Ferenc Karsai, Moritz Humer, Espen Flage-Larsen, Peter Blaha, and Georg Kresse. Effects of electron-phonon coupling on absorption spectrum: K edge of hexagonal boron nitride. *Physical Review B*, 98(23):235205, 2018.

[15] Carina Faber, Paul Boulanger, Claudio Attaccalite, Elena Cannuccia, Ivan Duchemin, Thierry Deutsch, and Xavier Blase. Exploring approximations to the g w self-energy ionic gradients. *Physical Review B*, 91(15):155109, 2015.

[16] Bartomeu Monserrat. Correlation effects on electron-phonon coupling in semiconductors: Many-body theory along thermal lines. *Physical Review B*, 93(10):100301, 2016.

[17] Carina Faber, Ivan Duchemin, Thierry Deutsch, Claudio Attaccalite, Valerio Olevano, and Xavier Blase. Electron–phonon coupling and charge-transfer excitations in organic systems from many-body perturbation theory. *Journal of Materials Science*, 47(21):7472–7481, 2012.

[18] Andrea Marini. Ab initio finite-temperature excitons. *Physical review letters*, 101(10):106405, 2008.

[19] Himani Mishra and Sitangshu Bhattacharya. Giant exciton-phonon coupling and zero-point renormalization in hexagonal monolayer boron nitride. *Physical Review B*, 99(16):165201, 2019.

[20] A Chernikov, V Bornwasser, M Koch, S Chatterjee, CN Böttge, T Feldtmann, M Kira, Stephan W Koch, T Wassner, S Lautenschläger, et al. Phonon-assisted luminescence of polar semiconductors: Fröhlich coupling versus deformation-potential scattering. *Physical Review B*, 85(3):035201, 2012.

[21] Edoardo Baldini, Adriel Dominguez, Letizia Chiodo, Evgeniia Sheveleva, Meghdad Yazdi-Rizi, Christian Bernhard, Angel Rubio, and Majed Chergui. Anomalous anisotropic exciton temperature dependence in rutile tio 2. *Physical Review B*, 96(4):041204, 2017.

[22] Yatendra Pal Varshni. Temperature dependence of the energy gap in semiconductors. *physica*, 34(1):149–154, 1967.

[23] A Surrente, AA Mitioglu, K Galkowski, W Tabis, DK Maude, and P Plochocka. Excitons in atomically thin black phosphorus. *Physical Review B*, 93(12):121405, 2016.

[24] Cesar EP Villegas, AR Rocha, and Andrea Marini. Anomalous temperature dependence of the band gap in black phosphorus. *Nano letters*, 16(8):5095–5101, 2016.

[25] J Pollmann and H Büttner. Effective hamiltonians and bindings energies of wannier excitons in polar semiconductors. *Physical Review B*, 16(10):4480, 1977.

[26] Paolo Umari, Edoardo Mosconi, and Filippo De Angelis. Infrared dielectric screening determines the low exciton binding energy of metal-halide perovskites. *The Journal of Physical Chemistry Letters*, 9(3):620–627, 2018.

[27] RJ Elliott. Intensity of optical absorption by excitons. *Physical Review*, 108(6):1384, 1957.

[28] Walter Kohn and Lu Jeu Sham. Self-consistent equations including exchange and correlation effects. *Physical review*, 140(4A):A1133, 1965.

[29] Paolo Giannozzi, Stefano Baroni, Nicola Bonini, Matteo Calandra, Roberto Car, Carlo Cavazzoni, Davide Ceresoli, Guido L Chiarotti, Matteo Cococcioni, Ismaila Dabo, et al. Quantum espresso: a modular and open-source software project for quantum simulations of materials. *Journal of physics: Condensed matter*, 21(39):395502, 2009.

[30] Neil W Ashcroft, N David Mermin, et al. Solid state physics [by] neil w. ashcroft [and] n. david mermin., 1976.

[31] A Pishtshev and N Kristoffel. Understanding the electron-phonon interaction in polar crystals: Perspective presented by the vibronic theory. In *Journal of Physics. Conference Series (Online)*, volume 833, 2017.

[32] Ryan James Hunt, Bartomeu Monserrat, Viktor Zólyomi, and ND Drummond. Diffusion quantum monte carlo and g w study of the electronic properties of monolayer and bulk hexagonal boron nitride. *Physical Review B*, 101(20):205115, 2020.